EXPERIMENTAL IMMUNOLOGY

SCANDINAVIAN JOURNAL OF
Immunology
AN INTERNATIONAL MONTHLY JOURNAL

WILEY

Mycobacterial antigens accumulation in foamy macrophages in murine pulmonary tuberculosis lesions: Association with necrosis and making of cavities

Syeda Mariam Riaz[1] | Gunnar Aksel Bjune[2] | Harald G. Wiker[3] | Lisbet Sviland[4,5] |
Tehmina Mustafa[1,6] (ID)

[1]Centre for International Health, Department of Global Public Health and Primary Care, University of Bergen, Bergen, Norway

[2]Department of Community Medicine, Institute of Health and Society, The Faculty of Medicine, University of Oslo, Oslo, Norway

[3]Department of Clinical Science, University of Bergen, Bergen, Norway

[4]Department of Clinical Medicine, University of Bergen, Bergen, Norway

[5]Department of Pathology, Haukeland University Hospital, Bergen, Norway

[6]Department of Thoracic Medicine, Haukeland University Hospital, Bergen, Norway

Correspondence
Tehmina Mustafa, Centre for International Health, Department of Global Public Health and Primary Care, University of Bergen, Bergen, Norway.
Email: Tehmina.Mustafa@uib.no

Abstract

Understanding mechanisms of cavitation in tuberculosis (TB) is the missing link that could advance the field towards better control of the infection. Descriptions of human TB suggest that postprimary TB begins as lipid pneumonia of foamy macrophages that undergoes caseating necrosis and fragmentation to produce cavities. This study aimed to investigate the various mycobacterial antigens accumulating in foamy macrophages and their relation to tissue destruction and necrosis. Pulmonary tissues from mice with slowly progressive TB were studied for histopathology, acid-fast bacilli (AFB) and presence of mycobacterial antigens. Digital quantification using Aperio ImageScope was done. Until week 12 postinfection, mice were healthy, and lesions were small with scarce AFB and mycobacterial antigens. Colony-forming units (CFUs) increased exponentially. At week 16-33, mice were sick, macrophages attained foamy appearance with an increase in antigens ($P < .05$), 1.5 log increase in CFUs and an approximately onefold increase in AFB. At week 37-41, mice started dying with a shift in morphology towards necrosis. A >20-fold increase in mycobacterial antigens was observed with only less than one log increase in CFUs and sevenfold increase in AFB. Secreted antigens were significantly ($P < .05$) higher compared to cell-wall antigens throughout infection. Focal areas of necrosis were associated with an approximately 40-fold increase in antigen MPT46, functionally active thioredoxin, and a significant increase in all secreted antigens. In conclusion, mycobacterial antigens accumulate in the foamy macrophages in TB lesions during slowly progressive murine pulmonary TB. Secreted antigens and MPT46 correlated with necrosis, thereby implying that they might trigger the formation of cavities.

1 | INTRODUCTION

Ending tuberculosis (TB) disease remains an unachieved objective for many countries with an estimated 10 million new cases reported in the year 2018. TB patients with cavities are a major source of disease transmission within a population. Interventions hindering cavity formation could significantly decrease bacterial load in a patient, reduce disease transmission and as a result can lead to a significant reduction in disease incidence.[1,2]

Experimental studies using various animal models have given useful insight into the immune pathogenesis of primary TB, characterized by the granulomatous immune response. This immune response is very effective in controlling infection, supported by the epidemiological studies showing that 90%-95% of the infected individuals never develop active TB disease.[3] However, there is a scarcity of information on the immune pathogenesis of postprimary TB which largely accounts for TB cavitation. Understanding the factors involved in tissue destruction and development of cavitation in postprimary TB may ultimately yield novel strategies for reducing disease transmission.

Studies based on human biopsy and autopsy material from the pre-antibiotic era, when the natural course of TB disease could be studied without interference from antibiotics, have given important insight into the immune pathogenesis of postprimary TB.[4-6] It is suggested to begin as endogenous lipid pneumonia of foamy macrophages accumulating *Mycobacterium tuberculosis (M tuberculosis)* antigens and host lipids, which can undergo necrosis forming caseous pneumonia with the onset of clinical disease. Caseous pneumonia eventually undergoes softening and fragmentation which is coughed out forming a cavity. With time, the cavity matures and forms a thin wall of fibrosis supporting the proliferation of large numbers of *M tuberculosis*.[7] The disease is restricted from dissemination to the rest of the lung and body by the effective granulomatous reaction surrounding the cavities. Thus, cavitation in TB does not result from the enlargement and liquefaction of granulomas rather it develops as an independent process where mycobacterial antigens accumulating in foamy macrophages seem to play a central role.

M tuberculosis is well known to affect human immunity for its benefit. *M tuberculosis* in macrophages inhibits the formation of phagolysosome, overcomes oxidative stress and prevents apoptosis.[8-13] These strategies help *M tuberculosis* to establish a nutrient-rich intracellular niche to asymptomatically accumulate antigens for months until the sudden onset of massive inflammation and necrosis. Few in vitro experimental studies implicate interaction between mycobacterial cord factor (trehalose 6,6 dimycolate) and host lipids as a trigger for the release of mycobacterial antigens and initiating inflammation.[14] However, which mycobacterial antigens accumulate in foamy macrophages is not known. In vivo studies in TB lesions and association of various *M tuberculosis* antigens with necrosis and tissue destruction are lacking.

A murine model from our laboratory mimics postprimary human TB in some aspects. The disease progresses for many months without clinical symptoms, then rapidly undergoes necrosis and kills its host like in humans. The pattern of inflammation is pneumonia of *M tuberculosis* infected foamy macrophages rather than granulomas. These similarities make it a useful animal model to study the pathology of postprimary TB. The study aimed to investigate this murine model further for the various mycobacterial antigens accumulating in foamy macrophages during infection and their association with tissue destruction and necrosis.

2 | MATERIALS AND METHODS

2.1 | Murine model of slowly progressive primary TB

The murine model using genetically homogeneous B6D2F1 hybrid mice has been described earlier.[15] B6D2F1 hybrid mice are a cross between C57BL/6, carrying Bcg susceptible gene (Bcgs), and the other (DBA2) with Bcg resistant gene (Bcgr). The F1 hybrid mice are more robust and resistant to disease with a longer life span as compared to the pure inbred strains by controlling the un-characterized deficiencies of a recessive genetic origin. A total of 260 mice at the age of approximately 12 weeks were inoculated through the intraperitoneal route with 1.5×10^6 colony-forming units (CFUs) of H37Rv strain of *M tuberculosis*. The relatively low dose of infection was used to allow chronic lung pathology to develop. The mice were followed up to 70 weeks postinfection. Three mice were sacrificed at 1, 2, 4 weeks and then at 4 weekly intervals up to week 41 and later at 52, 57 and 70 weeks. Until week 24, one lung of the sacrificed mouse was used for histopathology and the other lung was used for measuring CFUs. From week 29, different mice at the same time point were used for measuring CFUs and histopathology. Both lungs from one mouse were used for in situ studies, the left lung was fixed in 4% buffered formalin, and the right lung was frozen at $-70°C$. Seven characteristics were used for assessing the signs of illness in mice, namely body form (normal—thin cachectic), spine form (normal—lordosis or kyphosis), appearance of coat (flat—raised pelt), gait (flat—toeing), activity (active—passive), behaviour (running—immobile) and abdominal muscles (flat abdomen—guarding). These characteristics were assessed by one experienced biotechnician who was responsible for animal care. According to severity, each characteristic was given a score of 5 to 1; score 5 was taken as best and score 1 as worst. Mice were considered very sick if they had a score of 1 in four characteristics, including cachexia. The murine model has been developed with permission from the Norwegian Experimental Animal Board.[15]

TABLE 1 Primary antibodies, target antigens, immunogens and dilutions used for immunohistochemistry

Primary antibody	Target antigens	Immunogen	Study name	Dilution
Anti-BCG	Whole bacteria including secreted and cell-wall antigens. It detects heterogenous *Mycobacterium tuberculosis* antigens.	Sonicates of *M bovis* containing both secreted and cell-wall antigens.	BCG	1:4000
Anti-body against cell-wall antigens	Cell-wall antigens	Cell-wall antigens	Cell-wall antigens	1:2000
Total Secreted antigens				
Anti-*M Tuberculosis* secreted proteins	Directed against total secreted proteins present in culture filtrate (CF)	5 weeks old culture filtrate of *M tuberculosis* with minimal cell lysis.	Total secreted antigens	1:100
Individual secreted antigens				
Anti-MPT51	MPT51(Ag85D, fbpD, Rv3803c)	MPT51 antigen found in CF of *M tuberculosis*	MPT51 antigen	1:100
Anti-MPT53	MPT53(DsbE, RV2878c)	MPT53 antigen found in CF of *M tuberculosis*	Soluble secreted antigen MPT53	1:100
Anti-MPT63	MPT63 (Rv1926c)	MPT63 antigen found in CF of *M tuberculosis*	Immunogenic protein MPT63/ Antigen MPT63	1:100
Anti-MPT64	MPT64 (Rv1980c)	MPT64 antigen found in CF of *M tuberculosis*	Immunogenic protein MPT64/ Antigen MPT64	1:100
Other antigens				
Anti-MPT46	MPT46(Thioredoxin Trx C, Rv3914)	MPT46 antigen found in CF of *M tuberculosis*	Thioredoxin	1:100

Abbreviations: CF, Culture filtrate; MPT, proteins purified from *Mycobacterium tuberculosis*.

2.2 | Primary antibodies

Primary antibodies used in the study are listed in Table 1. All antibodies used in the study were in-house rabbit polyclonal, except for anti-BCG. Immunogens for these antibodies were bacterial sonicate for cell-wall antigens, or mycobacterial antigens extracted and purified from the 5-week-old culture fluid of *M tuberculosis* with minimal lysis, as described previously.[16,17] The immunogens might have acquired minor impurities while separation from culture fluid, preparation and deliverance. However, polyclonal antibodies produced by the immune system are largely directed towards dominant injected immunogen, thereby specificity of these antibodies is reliable and has been determined by earlier studies ([16,18,19]) Rabbit anti-bacillus Calmette-Guerin (anti-BCG) is a polyclonal antibody available from DAKO Immunoglobulins, Copenhagen, Denmark (code B124; lot 063B). All primary antibodies were titrated to get a comparable working dilution for each antibody.

2.3 | Histology, bacillary count and immunohistochemistry

A series of 5-μm sections were prepared from formalin-fixed paraffin-embedded tissue block using sliding microtome (Leica Biosystems). The sections were stained with haematoxylin and eosin, Ziehl-Neelsen (ZN) and immunohistochemistry (IHC). Haematoxylin and eosin and ZN were done on automated machines in the routine histology laboratory. CFUs were measured previously as described.[15] All steps of IHC were performed manually as described previously.[15] Briefly, after deparaffinization and rehydration, sections were boiled for 20 minutes in citrate buffer (PH 6) in a microwave oven for antigen retrieval. Tris-buffered saline was used for washing between each incubation step. Peroxidase block (Dako Denmark A/S) was applied for 15 minutes to block the activity of endogenous peroxidase. Serum-free protein block (Dako Denmark A/S) was applied for 12 minutes to prevent non-specific binding of the antibody to tissues. Primary antibody was applied for 60 minutes followed by secondary antibody, labelled polymer HRP anti-rabbit (Dako Denmark A/S), for 40 minutes. For visualizing antigens, 3-amino-9-ethyl carbazole (AEC) substrate chromogen was applied for 15 minutes. The sections were counterstained with Mayer's Haematoxylin (Dako 3309) and mounted with immuno-mount medium (Dako Denmark A/S). IHC was monitored by two negative controls and 1 positive control. Antibody diluent instead of primary antibody and a known non-TB lymph node biopsy were used as negative controls. A TB biopsy with high bacterial and *M tuberculosis* antigen load was used as a positive control.

2.4 | Evaluation and quantification of immunohistochemistry and Ziehl-Neelsen staining

Whole-slide digital images were obtained at × 40 resolution using Aperio ScanScope CS® Slide Scanner (Aperio Technologies Inc). For quantification, colour deconvolution (CD) algorithm of Aperio ImageScope software (Aperio Technologies Inc) was used. Tissue section area containing the lesion was annotated manually for quantification of IHC and ZN staining. The input parameter values used for IHC and ZN quantification are shown (Figure 1A,B). Colours of interest for IHC quantification were red for AEC (colour 1) and blue for haematoxylin (colour 2). Red, green and blue (RGB) values were adjusted for colour 1 and colour 2 and threshold levels were adjusted for weak, medium and strong intensities to avoid the error of reading non-specific staining as positive. To obtain the optic density (OD) values of RGB for positive colour (red), a small region of red colour was annotated, and default CD algorithm was run and OD values of RGB for the red colour were obtained. To adjust the input parameters to detect red colour as positive, OD values of RGB obtained were copied and added to our algorithm settings as input parameter values for colour 1. A similar procedure was repeated for negative stain. Results were presented as a percentage of positive pixels that are strongly, moderately and weakly stained in the total stained area. A score was used to account for the intensity of staining and calculated as; 1.0*(%Weak) + 2.0*(%Medium) + 3.0*(%Strong). Figure 1C,D shows the screenshot of the digital image and markup image produced when the slides were analysed, where red is strong positive, orange is medium positive, yellow is weak positive, and blue is negative. The intensity of positivity was taken as a proxy measure for the amount for antigens expression. Strong positive was taken as increased accumulation of antigens marked by rusty red granular staining.

For ZN quantification, the same steps were followed as described above for obtaining OD values of RGB for the positive reddish-purple stain of acid-fast bacilli and background stain of aniline blue. The results were measured in Percent Total Positive that was taken as a proxy for acid-fast bacilli (AFB) count.

2.5 | Statistical analysis

Non-parametric statistical analysis methods were used. Mann-Whitney test was used for comparison of two independent groups. Wilcoxon signed-rank test was used for comparison of two related samples. Spearman's rho was used for correlation analysis. All the analysis was performed using SPSS v25.

3 | RESULTS

3.1 | Histopathology

3.1.1 | Early small diffuse lesions (week 8-12)

During weeks 8 and 12, small lesions were visible. Lesion formation seemed to start around the peribronchiolar region with collection of macrophages and lymphocytes (Figure 2.1A). Usually, inflammatory cells were not present in alveolar spaces. Interstitial pneumonia was evident by thick alveolar septa containing inflammatory cells mainly monocytes and lymphocytes, and few neutrophils.

3.1.2 | Well-demarcated focal lesions (week 16-33)

With the course of infection, number, morphology and organization of macrophages changed. Focally organized lesions were seen with a clear demarcation between lesion areas and normal lung tissue, and with more defined distribution of macrophages separated from lymphocytes (Figure 2.1B). Lymphocytes formed tightly packed islets surrounded by foamy macrophages. Macrophages with large light staining nuclei and vacuolated eosinophilic cytoplasm were seen (Figure 2.1C). With the progression of infection, the macrophage dominated areas increased in size compared to lymphocyte areas. From week 33, early destructive changes could be seen in the macrophages evident by cell swelling, pyknotic bodies and karyorrhexis (Figure 2.1D). Neutrophils were seen adjacent to dying macrophages. Clusters of macrophages with destructive changes were seen in the alveolar space. Hyperplasia of bronchus-associated lymphoid tissue was also observed.

3.1.3 | Expansive lesions (week 37-41)

From week 37, a shift in disease severity was observed with an increase in mortality. The lesions expanded to occupy more than 80% of lung parenchyma. The expansive lesions contained more foamy macrophages and smaller number and size of lymphocytes aggregate as compared to well-demarcated lesions at earlier time points. Very sick mice were seen to contain more areas of focal necrosis in the lesions as compared to the less sick mice. Overall, mice in these weeks were grouped based on the lesion morphology and extent of necrosis as follows:

Expansive lesions with no necrosis: Four out of 10 mice had expansive lesions without necrosis. Lesions in these mice occupied most of the lung parenchyma but did not show
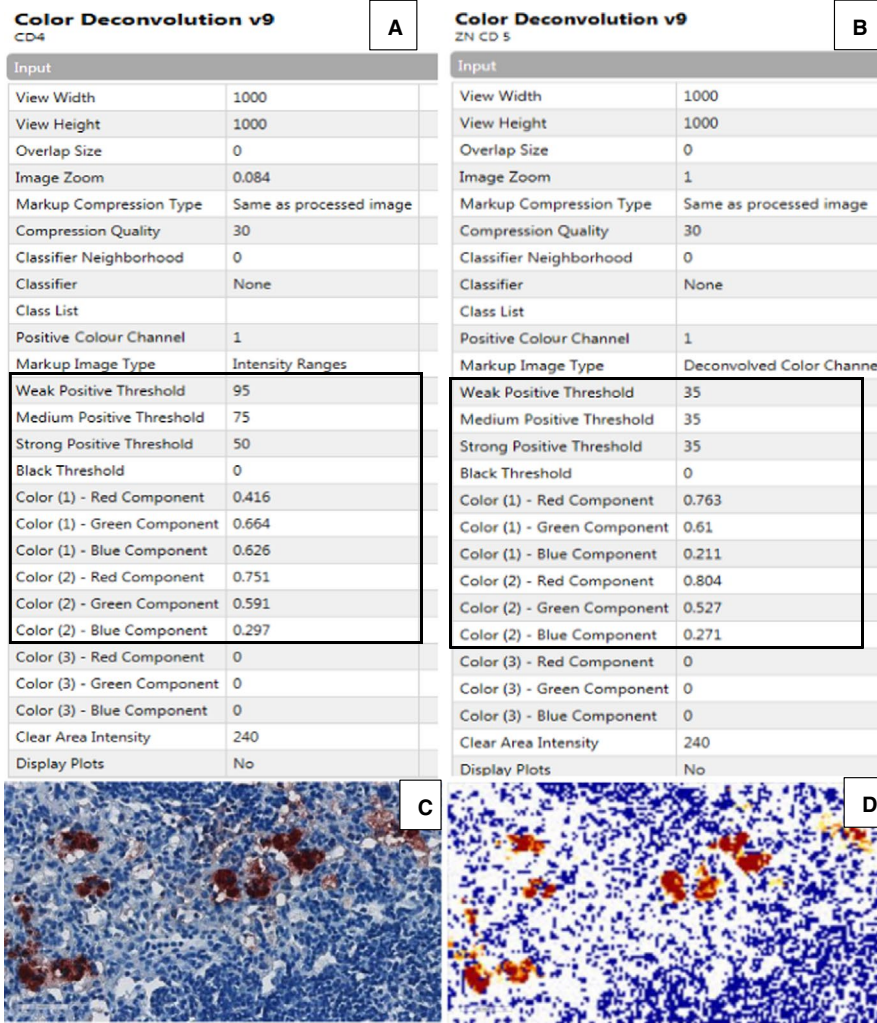
FIGURE 1 Input parameters used in immunohistochemistry (IHC) and Ziehl-Neelsen (ZN) quantification in colour deconvolution algorithm and screenshots of whole-slide digital images. A, Input parameter values used for IHC quantification, colour (1) detected the positive red colour for 3-amino-9-ethyl carbazole (AEC) substrate chromogen and colour (2) detected the negative background stained by haematoxylin. Weak, medium and strong positive thresholds measure different intensities of the same colour. B, Input parameters for ZN quantification, colour (1) detected reddish-purple colour of acid-fast bacilli and colour and (2) detected background blue stain. Weak, medium and strong positive thresholds values were kept constant as different intensities of colours were not required. C, Screenshot of whole-slide digital image where rusty red positive colour could be seen in varying intensities. D, Mark-up image for analysed slide where red is strong positive, orange is medium positive, and yellow is weak positive. Positivity was taken as proxy for amount of antigens accumulation. A and B, These pictures were taken as screenshot of input parameters of colour deconvolution algorithm of the Aperio Image Scope (v12.3.2.5030). C and D, These screenshots of whole-slide digital images taken from camera embedded in Aperio Image scope (v12.3.2.5030)

extensive destructive changes or areas of focal necrosis (Figure 2.1E). The bronchial epithelium in most cases was intact.
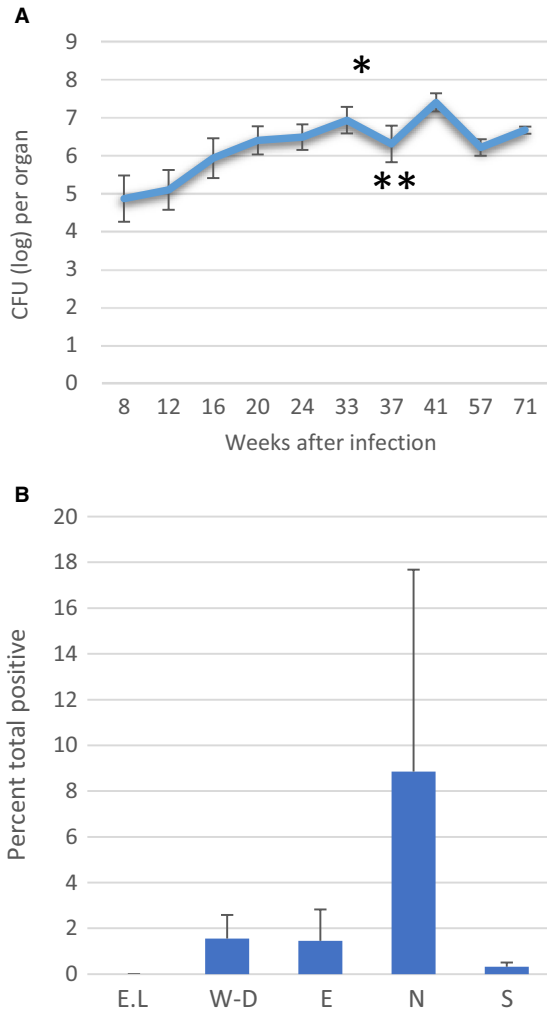
Expansive lesions with necrosis: Six out of 10 mice showed expansive lesions with necrosis. These lesions showed regions of focal necrosis (Figure 2.1F insert). Destructive changes involved most of the lesion area (Figure 2.1F). Completely sloughed off bronchial epithelium with cellular debris and proteinous material in the lumen could be seen. Two mice had complete bronchial occlusion. Lymphocytes islets were reduced in number and size. Normal-looking parenchyma surrounding the necrotic foci was infiltrated by neutrophils.

3.1.4 | Lesions in surviving mice (week 57-71)

By this time, most of the sick mice had died or sacrificed and relatively healthier mice survived. The lesions in these mice were also expansive and diffuse involving about 80% of lung parenchyma. The inflammatory cells consisted mainly of foamy macrophages and lymphocyte islets. As compared to previous expansive lesions, the lymphocyte islets were larger and were tightly packed (Figure 2.1G). Macrophages had a foamy appearance, the necrotic foci were visible; however, these areas were smaller than in the very sick mice mentioned above (Figure 2.1H). Bronchial
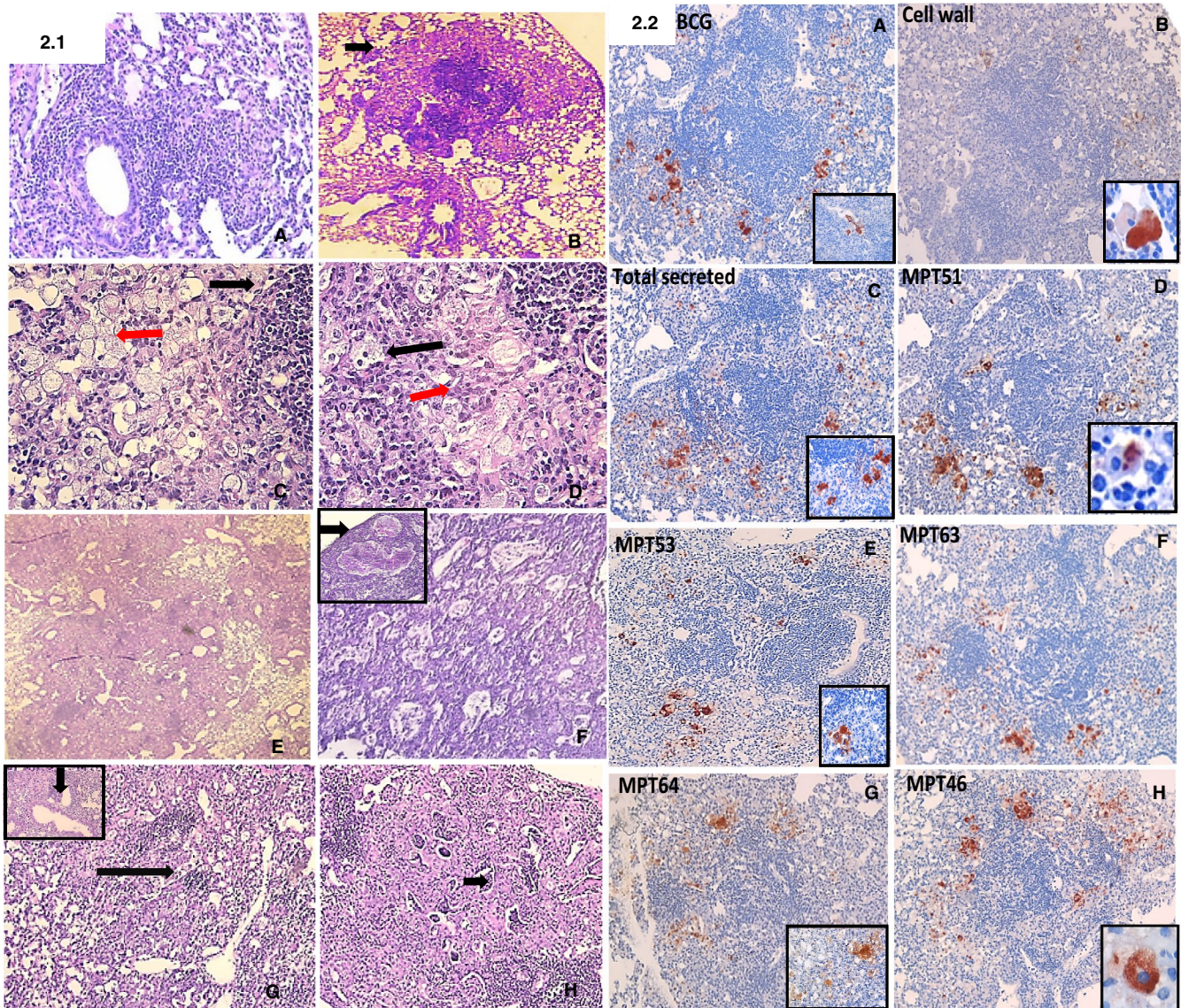
FIGURE 2 (2.1) Histopathology of lesions during slowly progressive tuberculosis as seen through light microscope. Three mice were sacrificed at each week, and one section from each mouse lung was stained with H&E. A, Early lesion starts to develop around peribronchiolar region (week 8-12). B, Well-demarcated lesion separated from normal lung parenchyma shown by the arrow (week 16-33) (×2.5). C, Tightly packed lymphocytes islets (black arrow) surrounded by foamy macrophages aggregate attaining increasingly vacuolated foamy appearance as the disease progresses (red arrow) (week 16-33) (×10). D, Early destructive changes could be seen in macrophages at week 33, pyknotic nuclei (black arrow) and karyorrhexis (red arrow) (week 16-33) (×63). E, Diffuse lesion occupying most of the lung parenchyma with no destructive changes or focal necrosis (week 37-41) (×2.5). F, Whole expansive lesion area with early destructive changes containing multiple foci of necrosis (arrow) (week 37- 41) (×10). (insert) extensive areas of focal necrosis were seen with necrosis. G, Lymphocytes islets in expansive lesion in surviving mice (×10), (insert) intact bronchial epithelium (week 57-71) (×10). H, Small areas of necrosis (arrow) could also be seen in surviving mice (week 57-71) (×10). (2.2) Immunohistochemistry showing expression pattern of various mycobacterial antigens in the formalin-fixed paraffin-embedded lung sections of mice with slowly progressive tuberculosis at week 16-33. The lesions at this stage of infection were well-demarcated and focal (×10). (A-insert) foamy macrophages containing antigens seen in clusters in alveolar space (×40). (B-insert) shows cytoplasmic granular staining (×63). (C-insert) shows granular staining filling the cytoplasm (×40). (D-insert) shows cytoplasmic focal staining (×40). (E-insert) shows macrophages present in alveolar space containing granular staining filling the cytoplasm (×10). (F) Macrophages in close vicinity of lymphocytes contained more antigens. (G-insert) showing granular cytoplasmic staining of different intensities in macrophages (×40). (H-insert) shows cytoplasmic granular staining seen in macrophages (×63). MPT: Proteins purified from *Mycobacterium tuberculosis*. Slides were viewed at microscope Leica DM 2000 LED and were taken with camera Leica MC 170 HD acquainted with software Leica Application Suite version 4.8.0 (build 154) Leica Microsystems Switzerland Limited

E.L: early lesion (8 – 12 weeks), **W-D**: well-demarcated lesion (16 – 33 weeks), **E**: expansive lesion without necrosis (37 – 41 weeks), **N**: expansive lesions with necrosis (37 – 41 weeks), **S**: survival (57 – 71 weeks)

FIGURE 3 Bacterial colony-forming units (CFUs) and acid-fast bacilli (AFB) during the slowly progressive tuberculosis. Lungs from three mice were used at each time point. A, CFUs of *M tuberculosis* in lungs during the weeks after infection. CFUs increased progressively until week 20. From week 33 onwards, the CFUs were rather stable with a significant increase (*$P < .05$) at week 41 corresponding to change in histopathology and mortality. CFUs were significantly (**$P < .05$) less in surviving mice at week 57 and 71. Error bars indicate confidence interval of the mean. B, The acid-fast count quantified as Percent Total Positive pixels in various types of lesion grouped according to lesion morphology. At each week, three mice were sacrificed and one section from each mouse lung was stained. The AFB increased from week 16 as the lesions became well-demarcated with macrophages and lymphocytes forming separate aggregates. An increase in count was observed corresponding to appearance of necrosis in lesions at week 37. Expansive lesion without foci of necrosis contained small amount of AFB. In the surviving mice at week 57-71, AFB count was noticeably low. Mann-Whitney test was used for comparison of two independent groups. Error bar indicates confidence interval of median. Graphs were made on SPSS and then modified graphically on word document

occlusion was not seen, and bronchial epithelium did not exhibit destructive change.

3.2 | Bacterial Colony-Forming Units (CFUs)

CFUs in the lungs of mice increased progressively until week 20 (Figure 3A). From week 33 onwards, the CFUs were rather stable. A significant increase ($P < .05$) at week 41 was observed with a sudden change in histopathology and mortality. CFUs were significantly ($P < .05$) less in mice at week 57 and 71.

3.3 | Acid-fast bacilli

Figure 3B shows the counts of acid-fast bacilli (AFB) in the pulmonary lesions of mice according to lesion morphology. AFB were seen mainly in the macrophages. The AFB increased as the lesions matured into well-demarcated lesions with macrophages and lymphocytes forming separate aggregates. A ninefold increase was observed in lesions containing necrotic foci. Expansive lesions without foci of necrosis contained small amounts of AFB. In the surviving mice, AFB count was noticeably low.

3.4 | Mycobacterial antigens

Figure 4 shows the various mycobacterial antigens during the infection. During week 8-12, expression of all antigens was low. From week 16, expression of all antigens increased. There was a significant positive correlation between all the antigens ($r < .05$; Table 2). BCG and cell-wall antigens were stable throughout the infection, while the total secreted antigens increased significantly at week 41, followed by a decline at later time points. The pattern of individual secreted antigens varied. Cell-wall antigens were lower and expressed weakly as compared to the total secreted antigens (Figure 5A,B).

All the antigens were seen in foamy macrophages with variable staining intensity (Figure 2.2). The pattern of staining was mainly granular in the cytoplasm (Figure 2.2 B, H). Some macrophages showed diffused granular staining filling the cytoplasm (Figure 2.2 C), and some had lesser focal staining in parts of the cytoplasm (Figure 2.2D) which could be indicative of antigens contained in the sub-cytoplasmic vacuoles. Within lesions, macrophages in close vicinity of lymphocytes were seen containing more antigens (Figure 2.2 F). Very often macrophages residing in alveoli of normal-looking parenchyma were also seen containing antigens.
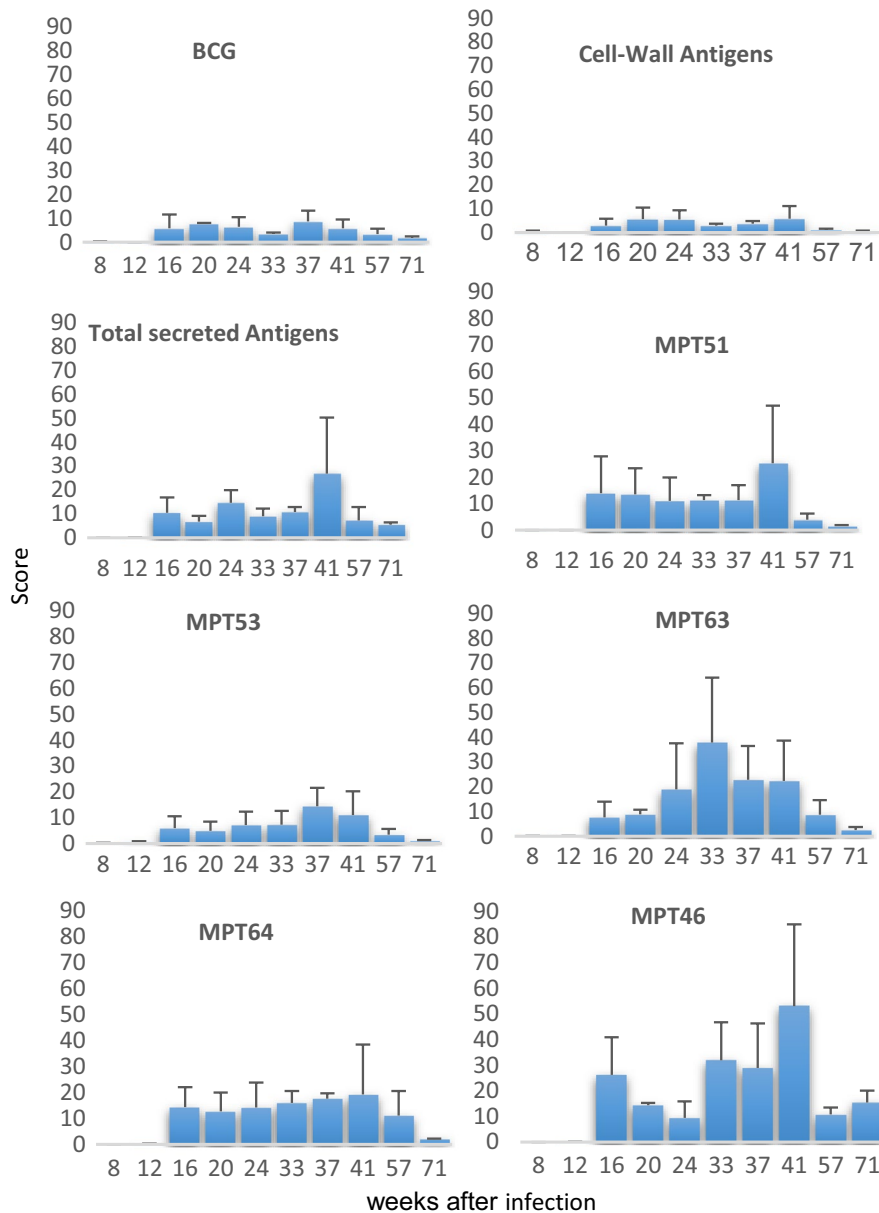
FIGURE 4 Expression of various mycobacterial antigens during the slowly progressive tuberculosis. Mycobacterial antigens were detected by immunohistochemistry in the formalin-fixed paraffin-embedded tissue sections. At each week, three mice were sacrificed and one section from each mouse lung was stained. The staining was quantified by colour deconvolution (CD) algorithm of Aperio ImageScope software. The antigens were measured as a percentage of positive pixels. A score was used to account for the intensity of staining and calculated as; 1.0*(%Weak) + 2.0*(%Medium) + 3.0*(%Strong). Wilcoxon signed-rank test was used for comparison of two related samples. Error bars indicate confidence of interval for the median. During week 8-12, expression of all antigens was low. From week 16, expression of all antigens increased. BCG and cell-wall antigens were stable throughout the course of the infection, while the total secreted antigens increased significantly at week 41, followed by a decline at later time points. The pattern of individual secreted antigens varied. Graphs were made on SPSS and then modified graphically on word document

3.5 | Mycobacterial antigens according to lesion morphology

Figures 5C and 6 show the mycobacterial antigen expression according to the lesion morphology. All antigens increased during the infection and in various lesions, but the magnitude of the increase was different. There was a significant difference ($P < .05$) in the expression of cell-wall, total secreted antigens and individual secreted antigens MPT51, MPT53, MPT63 and MPT46 with a change in the lesion morphology. BCG and MPT64 did not show a significant difference (Figure 5C). Expression of all antigens increased among well-demarcated focal lesions between weeks 16-33 ($P < .05$). Levels of secreted antigens were sixfold higher than cell-wall antigens. Among individual antigens, MPT46 was expressed at the highest level followed by MPT64.

Among expansive lesions with necrosis during week 37-41, expression of all antigens was significantly higher as compared to the lesions without necrosis ($P < .05$) except for MPT64, MPT46 and MPT53. In the necrotic lesions as compared to the non-necrotic lesion, the total secreted antigens increased to more than 20-fold whereas cell-wall antigens increased to < 10-fold. The pattern of staining intensities for cell wall and total secreted antigens was reverse, indicating more accumulation and higher amounts of secreted antigens as compared to cell-wall antigens (Figure 5A,B). The expression of BCG was like cell-wall antigens. Among individual secreted antigens, the expression of MPT46 was highest in these lesions.

Among the surviving mice at week 57-71, the expression of all antigens was significantly lower in the lesions as compared to the necrotic lesions ($P < .05$) except for MPT64.

TABLE 2 Correlation between various mycobacterial antigens, acid-fast bacilli and bacillary colony-forming units during the course of disease

	CFU	AFB	BCG	Cell-wall	Total secreted	MPT51	MPT53	MPT63	MPT64	MPT46
CFU	1.000[a]	0.230[a]	0.234[a]	0.368	0.319	0.362	0.400	0.454	0.454	0.381
AFB			0.599	0.556	0.449	0.554	0.505	0.513	0.518	0.416
BCG				0.847	0.740	0.871	0.784	0.820	0.668	0.675
Cell-wall					0.824	0.898	0.877	0.850	0.678	0.621
Total secreted						0.826	0.856	0.811	0.654	0.674
MPT 51							0.852	0.891	0.736	0.725
MPT 53								0.853	0.668	0.699
MPT 63									0.848	0.773
MPT 64										0.660

Note: The correlation between colony-forming units, acid-fast bacilli, expression of BCG antigens and total secreted antigens was not significant.

Abbreviations: AFB, acid-fast bacilli; CFU, colony-forming unit; MTP, proteins derived from *Mycobacterium tuberculosis*

[a]The correlation is not significant above 0.05 level.

MPT64 seemed to be expressed at relatively same level throughout the infection.

3.6 | Comparison of mycobacterial antigens with CFUs and AFB
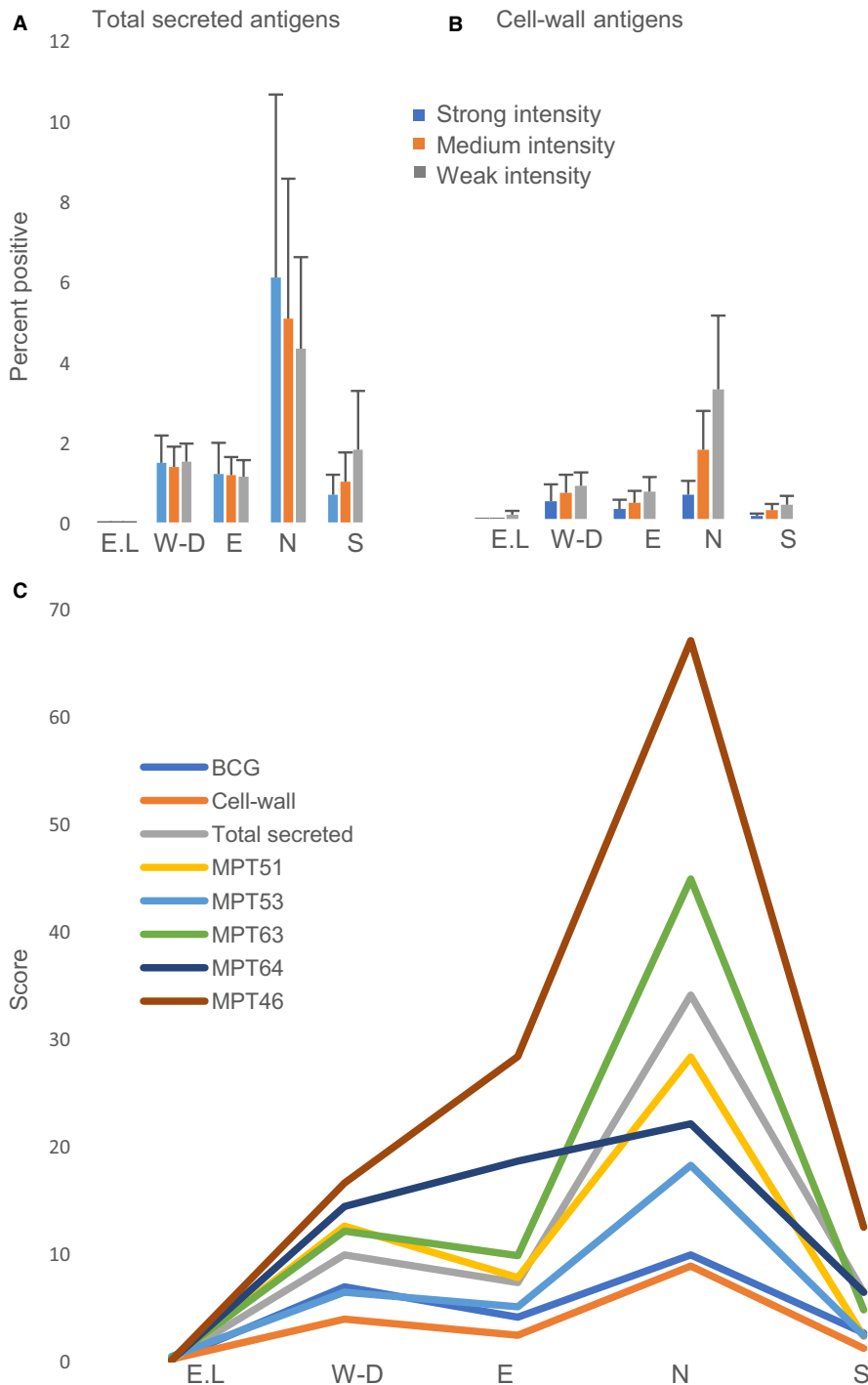
In the early small diffuse lesions, CFU increased but there was no increase in AFB and antigens. With the progression of infection when the lesions attained well-demarcated focal morphology, there was an increase in the levels of antigens, 1.5 log increase in CFU and an approximately onefold increase in AFB. With the shift in lesion morphology towards necrosis at week 37 and increased mortality, a >20-fold increase in mycobacterial antigens and an approximately sevenfold increase in AFB was in sharp contrast to the slight increase of less than one log in CFU. There was no significant correlation between CFU and total secreted antigens along the course of infection ($r > .05$; Table 2).

4 | DISCUSSION

We studied the expression pattern of various mycobacterial antigens in the murine pulmonary TB lesions and its association with the necrotic tissue pathology. A large increase in CFU was observed in the early stage with little or no antigen accumulation. Antigens started to accumulate in well-demarcated focal lesions with marked accumulation of MPT46 and secreted antigens. As the lesions expanded to more than 80% of the lung parenchyma, the necrosis of tissue was associated with increased mortality. Mycobacterial antigens accumulation in these necrotic lesions was many folds (secreted antigens by more than 20-fold and cell-wall antigens by approximately fivefold) as compared to the slight increase

in CFUs, and a moderate sevenfold increase in AFB. The extent of necrosis and accumulation of antigens was less in mice who had survived the infection at week 52 and 71 even though the inflammation had involved more than 80% of lung parenchyma. The tremendous increase in secreted mycobacterial antigens exclusively in necrotic lesions suggests a relation between the accumulation of secreted mycobacterial antigen and tissue destruction and disease severity.

A previous study on human material involving the pulmonary TB lesions with extensive pathology as compared to the tuberculous lymphadenitis with limited pathology shows similar findings of extensive accumulation of secreted mycobacterial antigens in the pulmonary lesions as compared to lymph nodes.[20] These findings lend support to the hypothesis that the accumulation of secreted mycobacterial antigens is associated with the necrosis and disease severity in pulmonary TB. Secreted antigens are the most immunogenic proteins expressed during active multiplication of mycobacteria and are linked to bacterial virulence.[21,22] In our study, the number of viable bacilli did not increase with an increase in the secreted antigens, indicating that antigens accumulate throughout the disease. It has been known since the time of Koch that the tissues around active TB lesions are extremely sensitive to injections of soluble mycobacterial antigens. This suggests that accumulation and release of mycobacterial antigens are critical stages of developing caseous necrosis. It has been hypothesized that foamy macrophages accumulate mycobacterial antigens in TB lesions and after reaching a certain threshold release the antigens leading to extensive inflammation, tissue destruction and necrosis.[11] Trigger for the release of antigens and inflammation is hypothesized to occurs by an interaction between trehalose 6,6-dimycolate (TDM) and host lipids. TDM has been proposed as the trigger due to its ability to acquire highly toxic monolayer configuration when it comes in contact with lipid

FIGURE 5 Comparison of different intensities of various mycobacterial antigens during slowly progressive tuberculosis. Mycobacterial antigens were detected by immunohistochemistry in the formalin-fixed paraffin-embedded tissue sections. Three mice were sacrificed at 4 weekly intervals up to week 41 and later at 52, 57 and 70 weeks. One section from each mouse lung was stained. The staining was quantified by colour deconvolution (CD) algorithm of Aperio ImageScope software. The antigens were measured as a percentage of positive pixels. Distribution of total secreted antigens (A) cell-wall antigens (B) as strong, medium and weak intensity signals according to lesion morphology. The signal intensity of total secreted antigens was stronger than the cell-wall antigens in all lesions. There was a significant difference ($P < .05$) in expression in well-demarcated lesions and expansive lesions with necrosis for both total secreted and cell-wall antigens. C, The comparison of differential expression pattern of various mycobacterial antigens according to lesion morphology. The expression of MPT 46 was highest among all antigens. Mann-Whitney test was used for comparison of two independent groups. Wilcoxon signed-rank test was used for comparison of two related samples. Graphs were made on SPSS and then modified graphically on word document

E.L: early lesion (8 – 12 weeks), **W-D**: well-demarcated lesion (16 – 33 weeks), **E:** expansive lesion (37 – 41 weeks), **N:** expansive lesions with necrosis (37 – 41 weeks), **S:** survival (57 – 71 weeks)

droplet.[14] In our study, accumulation of secreted mycobacterial antigens in the foamy macrophages implies their role in disease pathogenesis, disease severity, tissue destruction and necrosis.

Among all the antigens, MPT46 was the most abundantly expressed antigen throughout the course of infection.

Interestingly, there was a marked increase in expression corresponding with necrosis in the lesions. MPT46 is found in the culture filtrate of *M tuberculosis* but could not be categorized as secreted or non-secreted protein based on localization index and two-dimensional electrophoresis.[16,18] A study has demonstrated that MPT46 is functionally

FIGURE 6 Immunohistochemistry showing expression pattern of various mycobacterial antigens in the formalin-fixed paraffin-embedded lung sections of mice with slowly progressive tuberculosis at week 37-41, in expansive necrotic compared to expansive-non-necrotic lesions. At each week, three mice were sacrificed and one section from each mouse lung was stained. All antigens had a significant difference ($P < .05$) in expression in necrotic and non-necrotic lesions except for MPT 46, MPT 53 and MPT 64 ($\times$10). Mann-Whitney test was used for comparison of two independent groups. MPT: Proteins purified from *Mycobacterium tuberculosis*. Slides were viewed at microscope Leica DM 2000 LED and were taken with camera Leica MC 170 HD acquainted with software Leica Application Suite version 4.8.0 (build 154) Leica Microsystems Switzerland Limited
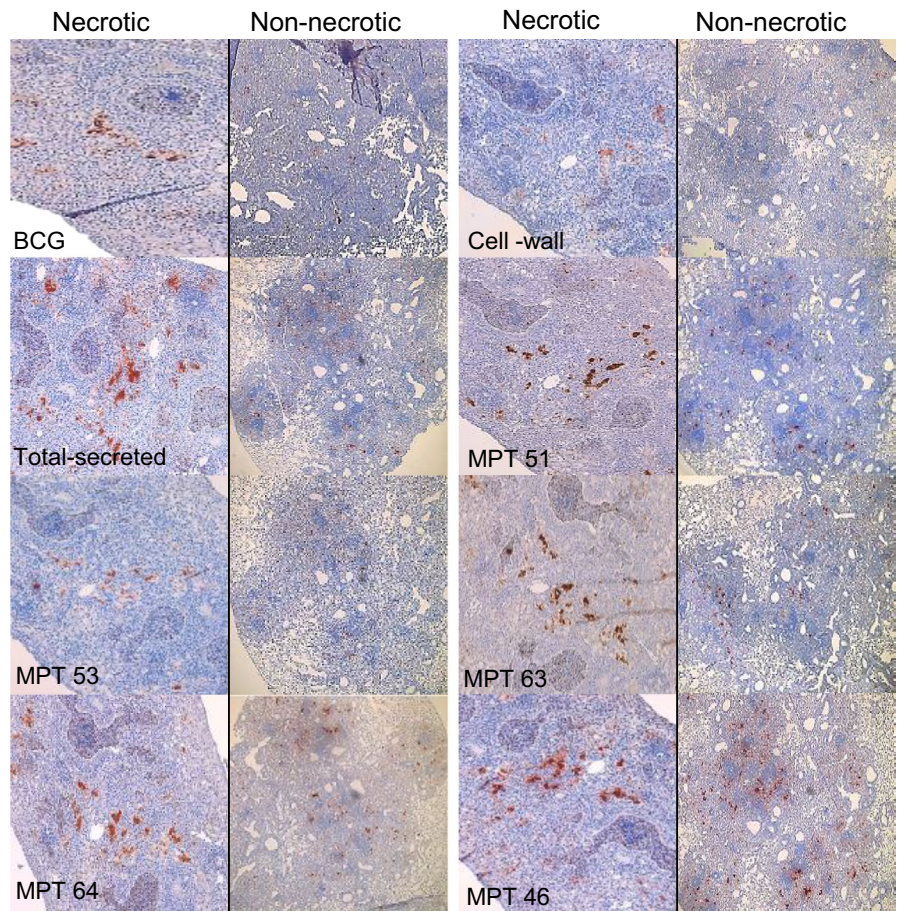
active thioredoxin of *M tuberculosis* and functions as active disulphide reductases. Thioredoxin plays an important role in cellular redox balance.[23,24] The thioredoxin system is involved in many important physiological functions including cellular DNA synthesis, protein repair, cellular protein disulphide reduction, detoxification of reactive oxygen species, and regulation of transcription factor and cell death pathways. For these reasons, it has been an attractive target for anti-tuberculous drugs.[25] Thioredoxin system is essential for the survival of *M tuberculosis* under oxidative stress as *M tuberculosis* lack antioxidant glutathione reductase system.[26,27] The genome of *M tuberculosis* encodes for three thioredoxins namely, thioredoxin A (Rv 1470), thioredoxin B (Rv 1471) and thioredoxin C (Rv 3914). MPT 49 is thioredoxin C. When tested for expression of thioredoxin gene in *M tuberculosis* in various growth conditions, thioredoxin C was expressed in all applied oxidative stress conditions.[24] Based on our findings, it can be hypothesized that *M tuberculosis* overexpresses thioredoxin in the stressful conditions of host immune response, and this protein accumulates in the foamy macrophages. At a certain threshold, cell lysis occurs, and the antigens are released. As shown earlier by "Koch phenomenon," the tissues around active TB lesions are extremely sensitive to mycobacterial antigens. The presence of large amounts of

antigens would lead to extensive inflammatory process, tissue destruction and formation of cavities, which is essential for bacterial survival by dissemination to new hosts.

Among individual secreted antigens, MPT63 was abundant in necrotic lesions. MPT63 is among the three most abundantly secreted antigens in culture filtrate of *M tuberculosis* and found only in *M tuberculosis* complex. The function of MPT63 is not known.[28,29] However, it is an immunogenic protein and its high expression in necrotic lesions suggests a role in *M tuberculosis* virulence. To what extent MPT63 induces necrosis and cavitation needs further studies.

The expression pattern of another secreted antigen MPT64 (Rv 1980c) was different from other secreted antigens. This antigen was expressed from week 16 and was constantly expressed throughout the course of the infection with no significant change related to lesion morphology. MPT64 is an actively secreted, immunogenic protein, found in culture filtrate of *M tuberculosis*.[30] The exact physiological function of MPT64 is not known. It is one of the predominant proteins among more than 33 actively secreted proteins and accounts for 8% of the total protein found in culture filtrate.[30] Loss of the gene region encoding for MPT64 from BCG progenitor has been correlated to drop in its virulence.[31] The accumulation of MPT64 over disease course and in granulomas

suggests a role in the persistence of chronic infection and *M tuberculosis* virulence, but probably not a major role in tissue destruction.

One limitation of the study is that the intensity of staining was used to measure the levels of antigens. All primary antibodies have been checked for their specificities, and each antibody was titrated on the tissues to get a comparable working dilution. This makes it possible to compare various antigen levels in this system based on the intensity of staining. However, this method gives only an approximation of the antigens levels and firm conclusion about the antigen levels cannot be drawn.

5 | CONCLUSION

This study shows that mycobacterial antigens accumulate in the foamy macrophages in TB lesions over the course of infection in slowly progressive murine pulmonary TB. The accumulation of secreted mycobacterial antigens and antigen MPT46 is correlated with necrosis, tissue destruction and mortality. Tissue destruction and necrosis is assumed as the precursor of cavitation, thereby implying a likely role of these antigens in the formation of cavities in TB disease.

CONFLICT OF INTERESTS
The authors declare that they have no financial and commercial conflict of interests.

AUTHOR CONTRIBUTIONS
Syeda Mariam Riaz did the laboratory work, data analysis and wrote the first draft. Tehmina Mustafa designed the project, acquired funds, contributed towards methodology development and data analysis, and was a major contributor in writing and editing the manuscript. Harald G Wiker contributed with the antibodies used in the study. Gunnar Aksel Bjune had contributed towards the development of mouse model earlier and contributed towards the write-up. Lisbet Sviland contributed towards write-up. All authors read and approved the final manuscript.

ORCID
Tehmina Mustafa https://orcid.org/0000-0001-9822-1191

REFERENCES
1. World Health Organization, 2018 Available from URL: https://www.who.int/tb/publications/global_report/en/.
2. Yoder MA, Lamichhane G, Bishai WR. Cavitary pulmonary tuberculosis: the Holy Grail of disease transmission. *Curr Sci*. 2004;86:74-81.
3. Lin PL, Flynn JL. Understanding latent tuberculosis: a moving target. *J Immunol*. 2010;185:15-22.
4. Rich AR. *The Pathogenesis of Tuberculosis*. 2nd edn. Springfield, IL: Charles C Thomas, 1951.
5. Canetti G. *The Tubercle Bacillus in the Pulmonary Lesion of Man: Histobacteriology and Its Bearing on the Therapy of Pulmonary Tuberculosis*. New York: Springer Publishing Company; 1955.
6. Medlar EM. The behavior of pulmonary tuberculous lesions; a pathological study. *Am Rev Tuberculosis*. 1955;71:1-244.
7. Canetti G, The J. Burns amberson lecture. *Am Rev Respir Dis*. 1965;92(5):687-703.
8. Mustafa T, Phyu S, Nilsen R, Bjune G, Jonsson R. Increased expression of Fas ligand on *Mycobacterium tuberculosis* infected macrophages: a potential novel mechanism of immune evasion by *Mycobacterium tuberculosis*? *Inflammation*. 1999;23(6):507-521.
9. Mustafa T, Wiker HG, Mørkve O, Sviland L. Reduced apoptosis and increased inflammatory cytokines in granulomas caused by tuberculous compared to non-tuberculous mycobacteria: role of MPT64 antigen in apoptosis and immune response. *Clin Exp Immunol*. 2007;150(1):105-113.
10. Ehrt S, Schnappinger D. Mycobacterial survival strategies in the phagosome: defence against host stresses. *Cell Microbiol*. 2009;11(8):1170-1178.
11. Hunter R, Actor J, Hwang S-A, et al. Pathogenesis and animal models of post-primary (bronchogenic) tuberculosis, a review. *Pathogens*. 2018;7(1):19.
12. Mustafa T, Bjune G, Jonsson R, Hernandez Pando R, Nilsen R. Increased expression of fas ligand in human tuberculosis and leprosy lesions: a potential novel mechanism of immune evasion in mycobacterial infection. *Scand J Immunol*. 2001;54(6):630-639.
13. Mogga S, Mustafa T, Sviland L, Nilsen R. Increased Bcl-2 and reduced Bax expression in infected macrophages in slowly progressive primary murine Mycobacterium tuberculosis infection. *Scand J Immunol*. 2002;56(4):383-391.
14. Hunter RL, Olsen MR, Jagannath C, Actor JK. Multiple roles of cord factor in the pathogenesis of primary, secondary, and cavitary tuberculosis, including a revised description of the pathology of secondary disease. *Ann Clin Lab Sci*. 2006;36(4):371-386.
15. Mustafa T, Phyu S, Nilsen R, Jonsson R, Bjune G. A mouse model for slowly progressive primary tuberculosis. *Scand J Immunol*. 1999;50(2):127-136.
16. Nagai S, Wiker HG, Harboe M, Kinomoto M. Isolation and partial characterization of major protein antigens in the culture fluid of *Mycobacterium tuberculosis*. *Infect Immun*. 1991;59(1):372-382.
17. Mustafa T, Wiker HG, Mfinanga SGM, Mørkve O, Sviland L. Immunohistochemistry using a *Mycobacterium tuberculosis* complex specific antibody for improved diagnosis of tuberculous lymphadenitis. *Mod Pathol*. 2006;19:1606.
18. Wiker HG, Harboe M, Nagai S. A localization index for distinction between extracellular and intracellular antigens of Mycobacterium tuberculosis. *Microbiology*. 1991;137(4):875-884.

19. Johnson S, Brusasca P, Lyashchenko K, et al. Characterization of the secreted MPT53 antigen of *Mycobacterium tuberculosis*. *Infect Immun*. 2001;69(9):5936-5939.

20. Mustafa T, Leversen NA, Sviland L, Wiker HG. Differential in vivo expression of mycobacterial antigens in *Mycobacterium tuberculosis* infected lungs and lymph node tissues. *BMC Infect Dis*. 2014;14(1):535.

21. Majlessi L, Prados-Rosales R, Casadevall A, Brosch R. Release of mycobacterial antigens. *Immunol Rev*. 2015;264(1):25-45.

22. Andersen P, Askgaard D, Ljungqvist L, Bentzon MW, Heron I. T-cell proliferative response to antigens secreted by *Mycobacterium tuberculosis*. *Infect Immun*. 1991;59(4):1558-1563.

23. Wieles B, Nagai S, Wiker HG, Harboe M, Ottenhoff T. Identification and functional characterization of thioredoxin of *Mycobacterium tuberculosis*. *Infect Immun*. 1995;63(12):4946-4948.

24. Akif M, Khare G, Tyagi AK, Mande SC, Sardesai AA. Functional studies of multiple thioredoxins from *Mycobacterium tuberculosis*. *J Bacteriol*. 2008;190(21):7087-7095.

25. Sweeney N, Lipker L, Hanson A, et al. Docking into *Mycobacterium tuberculosis* thioredoxin reductase protein yields pyrazolone lead molecules for methicillin-resistant *Staphylococcus aureus*. *Antibiotics*. 2017;6(1):4.

26. Kumar A, Farhana A, Guidry L, Saini V, Hondalus M, Steyn AJC. Redox homeostasis in mycobacteria: the key to tuberculosis control? *Expert Rev Mol Med*. 2011;13:e39.

27. Lu J, Holmgren A. The thioredoxin antioxidant system. *Free Radic Biol Med*. 2014;66:75-87.

28. Manca C, Lyashchenko K, Wiker HG, Usai D, Colangeli R, Gennaro ML. Molecular cloning, purification, and serological characterization of MPT63, a novel antigen secreted by *Mycobacterium tuberculosis*. *Infect Immun*. 1997;65(1):16-23.

29. Goulding CW, Parseghian A, Sawaya MR, et al. Crystal structure of a major secreted protein of *Mycobacterium tuberculosis*—MPT63 at 1.5-Å resolution. *Protein Sci*. 2002;11(12):2887-2893.

30. Chu TPJ, Yuann JMP. Expression, purification, and characterization of protective MPT64 antigen protein and identification of its multimers isolated from nontoxic *Mycobacterium tuberculosis* H37Ra. *Biotechnol Appl Biochem*. 2011;58(3):185-189.

31. Behr M, Wilson M, Gill W, et al. Comparative genomics of BCG vaccines by whole-genome DNA microarray. *Science*. 1999;284(5419):1520-1523.